PNAS
www.pnas.org

Supplementary Information for

ATP hydrolysis-coupled peptide translocation mechanism of Mycobacterium tuberculosis ClpB

Hongjun Yu, Tania J. Lupoli, Amanda Kovach, Xing Meng, Gongpu Zhao, Carl F. Nathan*, and Huilin Li*

* For correspondence: cnathan@med.cornell.edu or Huilin.Li@vai.org

This PDF file includes:

Figs. S1 to S6
Tables S1
Caption for movies S1

Other supplementary materials for this manuscript include the following:

Movies S1

www.pnas.org/cgi/doi/10.1073/pnas.1810648115

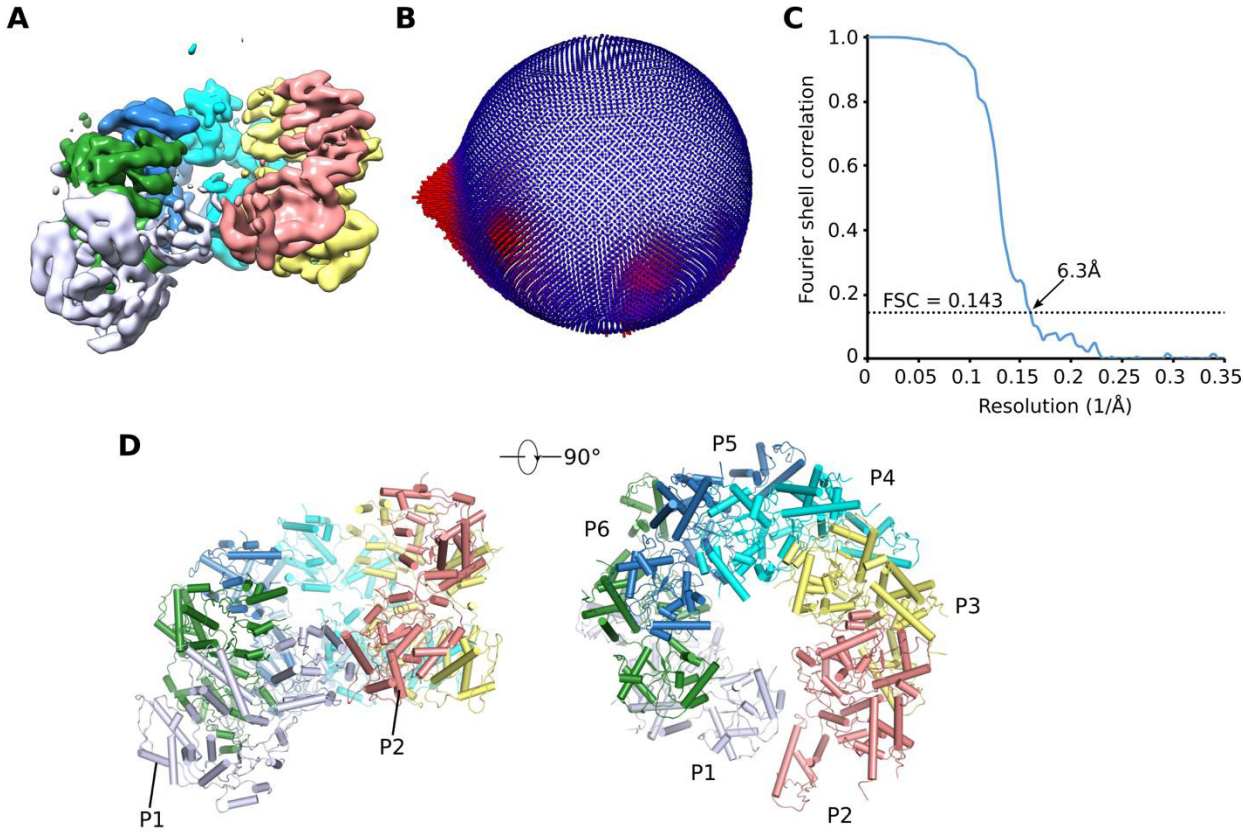

Fig. S1. Cryo-EM 3D reconstruction of *Mtb* ClpB in complex with AMPPNP. (**A**) 3D density map of ClpB complexed with AMPPNP. (**B**) Eulerian angle distribution of all particles used in the 3D reconstruction, shown in the same orientation as in panel **A.** (**C**) The gold-standard Fourier shell correlation (FSC) curve of the map. (**D**) A side view (left) and a top view (right) of the atomic model. The model was derived by rigid-body docking of the NBD1 and NBD2 structures of P5 promoter of *Mtb* ClpB Conformer 1.

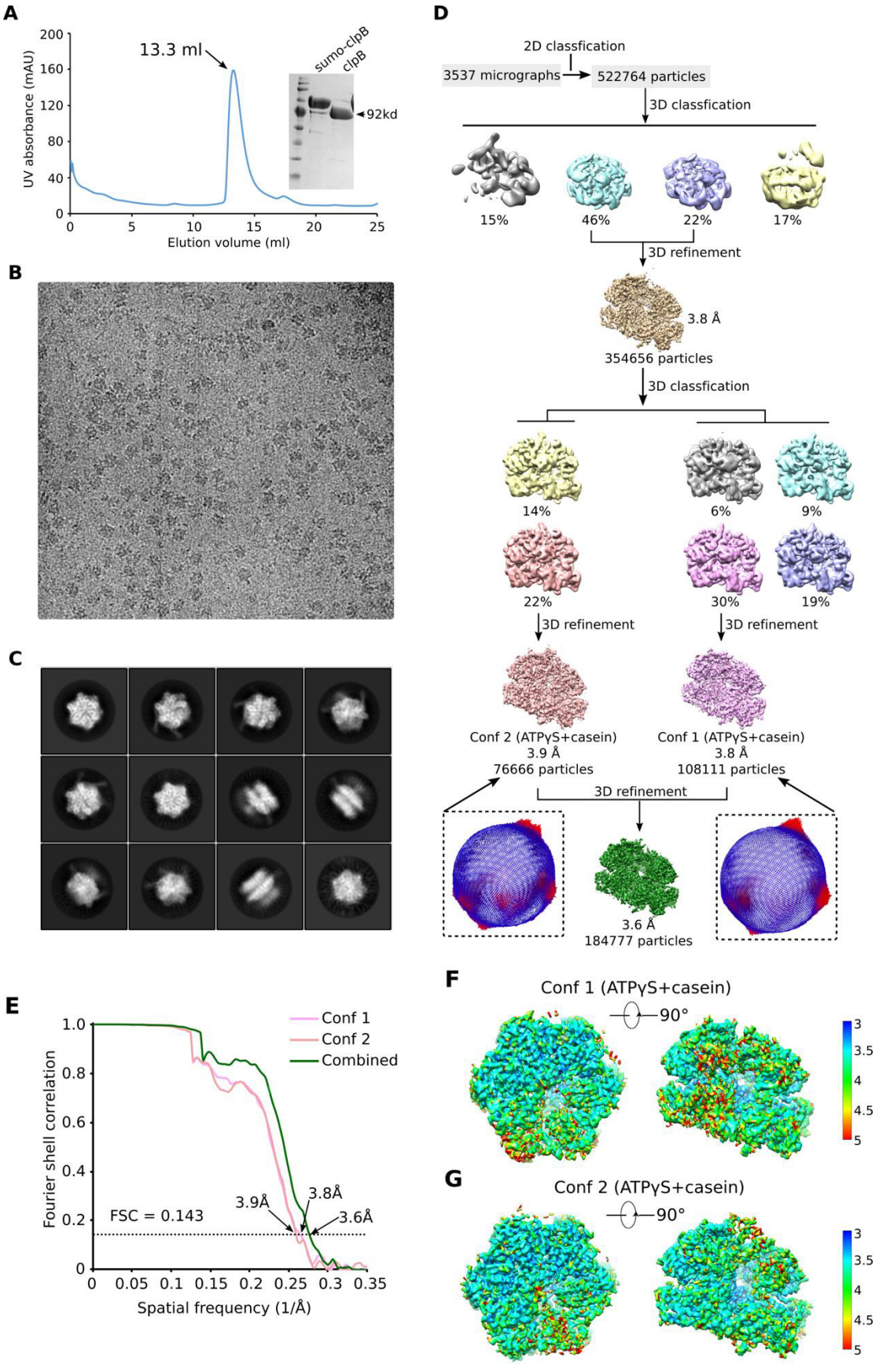
A
13.3 ml
sumo-clpB
clpB
92kd
UV absorbance (mAU)
Elution volume (ml)
B
C
D
2D classfication
3537 micrographs
522764 particles
3D classfication
15%
46%
22%
17%
3D refinement
3.8 Å
354656 particles
3D classfication
14%
6%
9%
22%
30%
19%
3D refinement
3D refinement
Conf 2 (ATPγS+casein)
3.9 Å
76666 particles
Conf 1 (ATPγS+casein)
3.8 Å
108111 particles
3D refinement
3.6 Å
184777 particles
E
Conf 1
Conf 2
Combined
Fourier shell correlation
FSC = 0.143
3.9Å
3.8Å
3.6Å
Spatial frequency (1/Å)
F
Conf 1 (ATPγS+casein)
90°
G
Conf 2 (ATPγS+casein)
90°

Fig. S2. Cryo-EM analysis of *Mtb* ClpB in complex of casein and ATPγS. (A) Gel filtration profile of ClpB (Superose 6 10/300 GL column). Inset is an SDS-PAGE of ClpB before and after removal of the sumo tag. (**B**) Representative cryo-EM micrograph. (**C**) Representative 2D class averages. (**D**) The work flow of cryo-EM data processing. Insets with dashed boxes are angular distribution of all particles used in the corresponding 3D reconstructions. (**E**) The gold-standard Fourier shell correlation (FSC) curve of the corresponding 3D maps. (**F-G**) Local resolution of the 3D density maps of Conformer 1 (**F**) and Conformer 2 (**G**), calculated with ResMap.

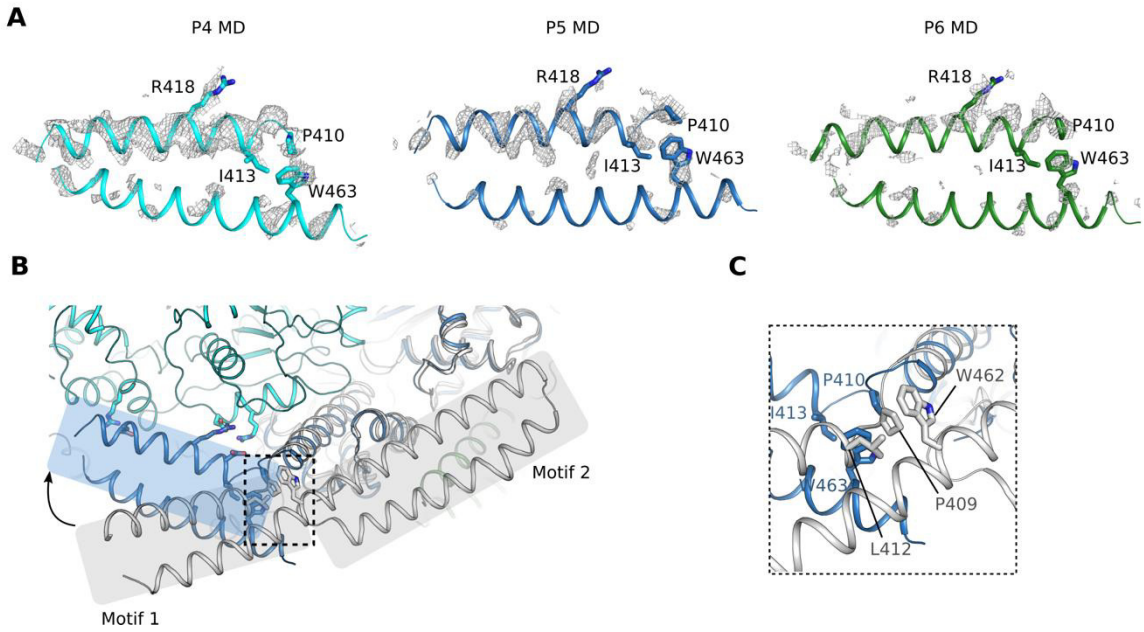

Fig. S3. Analysis of the MD conformations. (**A**) Cryo-EM density of motif 1 of the MD domains of 'tight' protomers P4, P5 and P6 in Conformer 1. The structure of MD motif 1 extracted from the crystal structure of *E. coli* ClpB (PDB ID 4CIU), 56% identical to the *Mtb* protein, fitted well in this density as a rigid-body. (**B**) The MD domain motif 1 of protomer P5 (blue) adopted a conformation that interacts with adjacent protomer P4 while its MD motif 2 was dynamic. An *E. coli* ClpB protomer structure in the MD motif 1-unbracing form (PDB ID 4CIU; grey) was superimposed on NBD1 of P5 (blue) of *Mtb* ClpB. This comparison showed that a rotation around the central hydrophobic region between motifs 1 and 2 interconverted the unbracing and bracing forms of the MD motif 1. (**C**) An enlarged view of the hydrophobic region in the MD domain, highlighted by a dashed box in panel **B**.

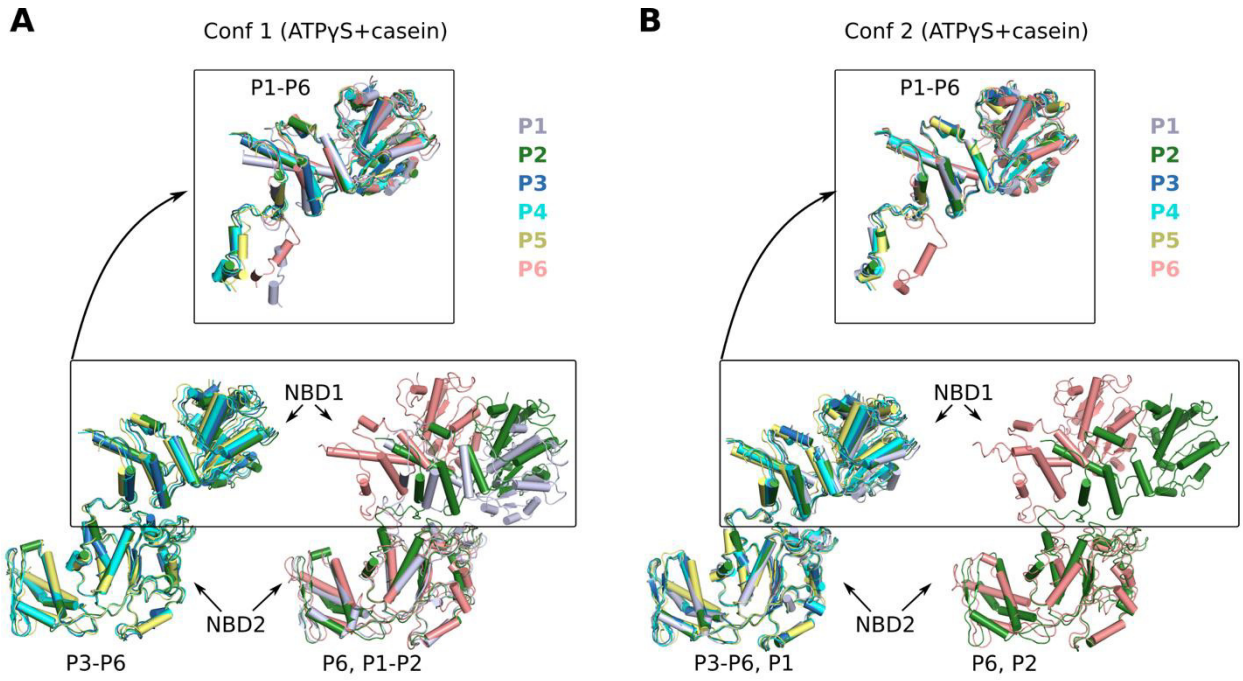

Fig. S4. Conformational differences among individual protomers of *Mtb* ClpB. (**A**) Conformer 1. (**B**) Conformer 2. Bottom, the six protomers were aligned by their respective NBD2 domains. The NBD2 domains of the six protomers in both conformers were superimposable. The NBD1 domains of P1-P2 in Conformer 1 (**A**) and NBD1 of P2 in Conformer 2 (**B**) moved the most among the six protomers. Top, in both Conformer 1 and 2, the NBD1 domains of all six protomers could be superposed among themselves. These comparisons indicated that the individual NBD1 and NBD2 domain structures were largely unchanged; the conformational differences were due to rigid-body motions of these NBD1 and NBD2 domains.

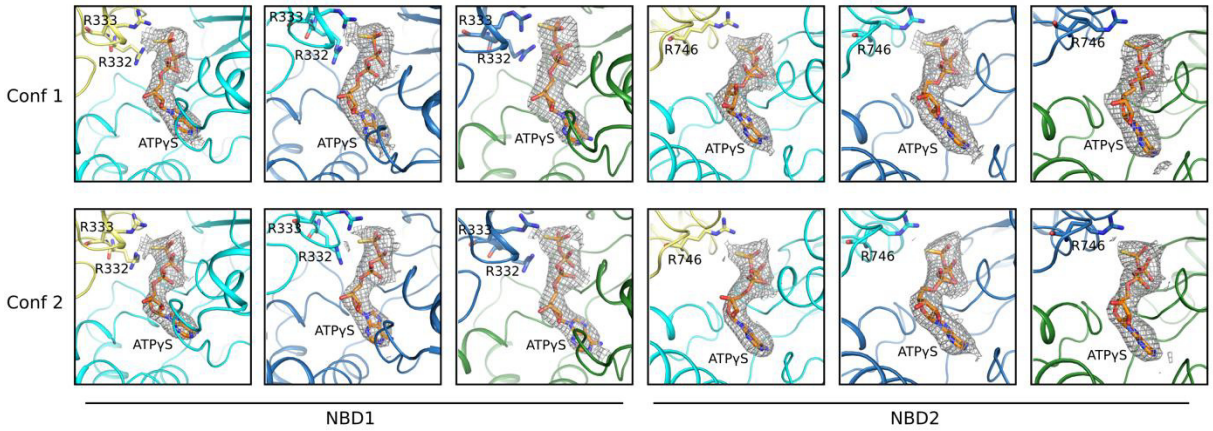

Fig. S5. Nucleotide states of protomers P4, P5 and P6 in Conformer 1 and 2.
Bound ATPγS in their NBD1 and NBD2 were superposed with densities displayed at the same threshold as that in **Fig. 5C**.

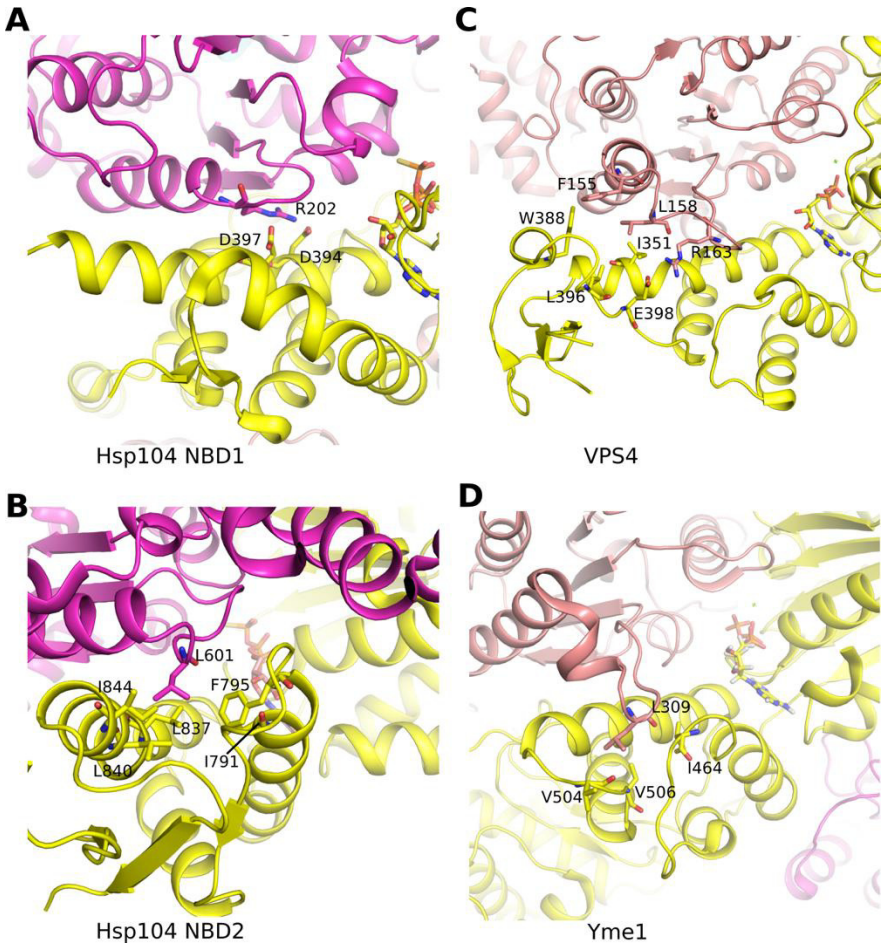

Fig. S6. The inter-protomer interactions outside the nucleotide sites in *Mtb* ClpB were similar to those of several other peptide-translocation ATPases. (**A, B**) NBD1 and NBD2 domains of Hsp104 (PDB ID 5VJH); (**C**) VPS4 (PDB ID 6AP1); (**D**) Yme1 (PDB ID 6AZ0). These inter-protomer interactions were of similar topologies and involved two similarly positioned moieties: (1) one or two α-helices of the small helical domain adjacent to the nucleotide binding site; (2) a loop connected to the β-stand preceding the Walker A motif of an adjacent protomer.

Table S1. Cryo-EM data collection parameters and structure refinement statistics.

Ligands complexed with *Mtb*ClpB	ATPγS+Casein Combined*	ATPγS+Casein Conformer 1	ATPγS+Casein Conformer 2	AMPPNP
EMDB ID	EMD-9027	EMD-7942	EMD-7943	EMD-9028
PDB ID	-	6DJU	6DJV	6ED3
Data collection				
Microscope		FEI Titan Krios		
Voltage (kV)		300		
Detector		Gatan K2 Summit		
Electron dose ($e^-/Å^2$)		52		
Pixel size (Å)		1.07		
Defocus range (μm)		1.1-3		
Reconstruction				
Software	RELION 2.0	RELION 2.0	RELION 2.0	RELION 2.0
Particles for final refinement	184,777	108,111	76,666	112,043
Final Resolution (Å)	3.6	3.8	3.9	6.3
Map-sharpening B factor ($Å^2$)	-127.0	-121.2	-128.3	-244.1
Model composition				
Protein chains		7	7	
Protein residues		3455	3481	
Nucleotides		12	12	
R.m.s. deviations				
Bond lengths (Å)		0.007	0.006	
Bond angles (°)		1.139	1.099	
Ramachandran plot				
Favored (%)		86.4	87.1	
Outlier (%)		0.6	0.4	
Validation				
Molprobity score		1.9	1.9	
Rotamer outlier (%)		0.9	0.7	
Clashscore		6.0	6.2	

*Atomic model was not built because of the mixed states of mobile protomers P1 and P2 (**Fig. 1C-D**).

Movie S1. Atomic trajectories of substrate translocation by *Mtb* ClpB. The movie was made by morphing from Stage 1 to Stage 2 and subsequently from Stage 2 to Stage 3 as illustrated in **Fig. 6B**.